within regions of the surface layer.

Acknowledgments

We are grateful to Louis Dall'Aglio for machining the calorimeter assembly, to Dr. Bonner Denton for his advice on the calorimeter–computer interface, and to Dr. Giorgio Careri, of the University of Rome, Dr. Enrico Gratton, of the University of Illinois, and Dr. F. R. Salemme, of the University of Arizona, for numerous stimulating discussions. A North Atlantic Treaty Organization research grant (1336) made possible a collaboration between Drs. Careri, Gratton, Salemme, and ourselves that led to the picture of the hydration process used above in interpreting the heat capacity results. Dr. Walter Kauzmann has made thoughtful and much appreciated comments, which have produced a more intelligible discussion of these results.

References

Benson, S. W., & Richardson, R. L. (1955) *J. Am. Chem. Soc. 77*, 2585–2590.
Berezin, G. I., Kiselev, A. V., & Sinitzyn, V. A. (1973) *J. Chem. Soc., Faraday Trans. 1 69*, 614–619.
Bull, H. B., & Breese, K. (1968) *Arch. Biochem. Biophys. 128*, 497–502.
Careri, G., Giansanti, A., & Gratton, E. (1979) *Biopolymers* (in press).
Cox, D. J., & Schumaker, V. N. (1961) *J. Am. Chem. Soc. 83*, 2439–2445.
Fujita, Y., & Noda, Y. (1978) *Bull. Chem. Soc. Jpn. 51*, 1567–1568.
Haly, A. R., & Snaith, J. W. (1968) *Biopolymers 6*, 1355–1377.
Haly, A. R., & Snaith, J. W. (1971) *Biopolymers 10*, 1681–1699.
Hill, T. L. (1949) *J. Chem. Phys. 17*, 762–771.
Hilton, B. D., Hsi, E., & Bryant, R. G. (1977) *J. Am. Chem. Soc. 99*, 8483–8490.
Hnojewyj, W. S., & Reyerson, L. H. (1959) *J. Phys. Chem. 63*, 1653–1654.
Hnojewyj, W. S., & Reyerson, L. H. (1961) *J. Phys. Chem. 65*, 1694–1698.
Horn, W. R., & Mennie, J. H. (1935) *Can. J. Res. 12*, 702–706.
Hutchens, J. O., Cole, A. G., & Stout, J. W. (1969) *J. Biol. Chem. 244*, 26–32.
Imoto, T., Johnson, L. N., North, A. C. T., Phillips, D. C., & Rupley, J. A. (1972) *Enzymes, 3rd Ed. 7*, 665–868.
Konicek, J., Suurkuusk, J., & Wadsö, I. (1971) *Chem. Scr. 1*, 217–220.
Kuntz, I. D., & Kauzmann, W. (1974) *Adv. Protein Chem. 28*, 239–345.
Lee, B., & Richards, F. M. (1971) *J. Mol. Biol. 55*, 379–400.
Leeder, J. D., & Watt, I. C. (1974) *J. Colloid Interface Sci. 48*, 339–344.
Millero, F. J., Ward, G. K., & Chetirkin, P. (1976) *J. Biol. Chem. 251*, 4001–4004.
Privalov, P. D., & Khechinashvili, N. N. (1974) *J. Mol. Biol. 86*, 665–684.
Richards, F. M. (1977) *Annu. Rev. Biophys. Bioeng. 6*, 151–176.
Rüegg, M., Moor, U., & Blanc, B. (1975) *Biochim. Biophys. Acta 400*, 334–342.
Rupley, J. A. (1969) *Biol. Macromol. 2*, 291–352.
Shrake, A., & Rupley, J. A. (1973) *J. Mol. Biol. 79*, 351–371.
Suurkuusk, J. (1974) *Acta Chem. Scand., Ser. B 28*, 409–417.
Suurkuusk, J., & Wadsö, I. (1974) *J. Chem. Thermodyn. 6*, 667–679.

Cooperative Binding of a Platinum Metallointercalation Reagent to Poly(A)·Poly(U)†

Jacqueline K. Barton and Stephen J. Lippard*

ABSTRACT: The cationic complex (2-hydroxyethanethiolato)(2,2′,2″-terpyridine)platinum(II), [(terpy)Pt(HET)]$^+$, binds cooperatively to poly(A)·poly(U) by intercalation. The melting temperature of poly(A)·poly(U) in low-salt buffer is increased by 6 °C in the presence of [(terpy)Pt(HET)]$^+$, indicating stabilization of the duplex structure by the bound platinum reagent. Viscosity measurements provide evidence for comparable lengthening of the polynucleotide in the presence of [(terpy)Pt(HET)]$^+$ and the intercalating dye, ethidium bromide. Scatchard plots of the binding of [(terpy)Pt(HET)]$^+$ to poly(A)·poly(U) and poly(I)·poly(C), determined through ultracentrifugation pelleting methods, show large positive curvature, reflecting the strong cooperativity associated with the platinum complex–RNA interaction. The characteristics of the binding isotherms are interpreted in terms of a model where cooperative pair units of [(terpy)Pt(HET)]$^+$ intercalate into the double-stranded polymer. At saturation, two platinum molecules are bound for every three base pairs. This stoichiometry may be compared with the nearest-neighbor-exclusion binding observed previously in the interaction of [(terpy)Pt(HET)]$^+$ and the ethidium cation with DNA, in which one intercalator occupies every other interbase-pair site at saturation. The striking differences observed in the interaction of [(terpy)Pt(HET)]$^+$ with DNA and RNA suggest that drug recognition is sensitive to the constraints imposed by nucleic acid secondary structure.

There have been extensive studies of the binding of aromatic heterocyclic dyes (Figure 1) to duplex DNA. The primary mode of interaction, first proposed by Lerman (1961), involves intercalation, where the cationic dye inserts between adjacent base pairs of the polynucleotide. The changes in physical properties that accompany the binding of dyes to double-stranded RNAs have also been interpreted in terms of an intercalation model (LePecq & Paoletti, 1967; Waring, 1961; Aktipis & Martz, 1974; Schmechel & Crothers, 1971; Zama

† From the Department of Chemistry, Columbia University, New York, New York 10027. *Received January 10, 1979.* This work was supported by National Institutes of Health Research Grant CA-15826 from the National Cancer Institute and by a National Science Foundation Predoctoral Fellowship to J.K.B.

0006-2960/79/0418-2661$01.00/0

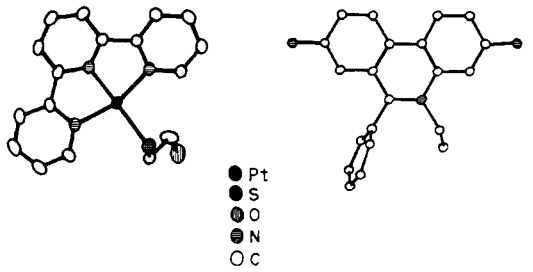

FIGURE 1: Molecular structures of (left) (2-hydroxyethanethiolato)(terpyridine)platinum(II) and (right) ethidium, two cationic intercalators employed in the present study.

& Ichimura, 1976; Douthart et al., 1973). Among the effects observed are changes in (1) the spectral properties and melting temperature of poly(A)·poly(U) upon binding of ethidium bromide (EtdBr;[1] Figure 1) (Aktipis & Martz, 1974); (2) the hydrodynamic properties of poly(A)·poly(U) upon binding of proflavin (Schmechel & Crothers, 1971); (3) the circular dichroism of acridine orange induced upon binding to double-stranded RNA and tRNA (Zama & Ichimura, 1976); and (4) a number of the physical properties upon ethidium binding to a naturally occurring, double-stranded RNA isolated from a mycophage (Douthart et al., 1973). The specific release of ribosomal proteins by nucleic acid intercalating agents has also been reported (Ballesta et al., 1976). A unique, strong EtdBr binding site exists in yeast $tRNA^{Phe}$, the nature of which has been a subject of debate. High-resolution NMR spectroscopic (Kearns & Jones, 1975; Jones et al., 1976) and fluorescence energy transfer studies (Wells & Cantor, 1977) indicated that EtdBr intercalates between tRNA base pairs AU_6 and AU_7. Recent crystallographic studies (Liebman et al., 1977) of the EtdBr–tRNA complex, however, revealed a nonintercalative mode of ethidium binding. The fact that ethidium binds strongly to only one site of the native $tRNA^{Phe}$ reflects the constraints of the tRNA tertiary structure.

During the course of work in this laboratory designed to provide heavy-metal labels for thiolated bases of polynucleotides (Heitner et al., 1972; Sunshine & Lippard, 1974), the interaction of $[(terpy)PtCl]^+$ with unfractionated *Escherichia coli* tRNA was investigated (Jennette, 1975). The results suggested that intercalation of the platinum complex, with concomitant disruption of the tertiary structure of the tRNA, exposed the thiocarbonyl moiety of s^4U_8, permitting platinum–sulfur bond formation. Subsequent studies of the binding of a related, substitutionally inert platinum complex, $[(terpy)Pt(HET)]^+$, with calf thymus DNA (Jennette et al., 1974) demonstrated that such heavy-metal complexes can function as intercalators. The stereochemical and electronic requirements for the intercalative binding of a variety of platinum-containing metallointercalation reagents have been examined (Howe-Grant et al., 1976; Lippard et al., 1976).

X-ray fiber diffraction studies (Lippard et al., 1976; Bond et al., 1975) of $[(terpy)Pt(HET)]^+$ and related complexes bound intercalatively to calf thymus DNA strongly support the nearest-neighbor-exclusion binding model in which every other interbase-pair site is occupied at saturation (Cairns, 1962; Crothers, 1968). The absence of fiber diffraction maxima from an ordered polynucleotide backbone precluded more detailed modeling of the intercalation site geometry. The intercalative binding of the platinum complexes to DNA is not cooperative, even though subject to the nearest-neighbor-exclusion effect. The study of a highly ordered intercalated polynucleotide complex by fiber X-ray diffraction techniques with dye bound in a cooperative fashion would probably allow the elucidation of the sugar phosphate conformational parameters of the helix at the intercalation site. We therefore became interested in investigating cooperative binding of intercalators to nucleic acids. A highly cooperative interaction between EtdBr and poly[d(G-C)] in very high (>4M) salt buffer had been reported (Pohl et al., 1972). The cooperative nature of the interaction appears to be a consequence of a salt-induced conformational change in the polymer that is reversed upon the intercalative binding of ethidium. A slight increase in the cooperativity associated with the binding of EtdBr to a variety of synthetic DNAs having a repetitive helix structure has also been observed (Bresloff, 1974; Crothers, personal communication).

It appears (Bresloff, 1974; Crothers, personal communication) that EtdBr binds to synthetic RNAs with neighbor exclusion constraints differing from those imposed by DNAs. In particular, ethidium binds intercalatively to double-stranded RNAs with a maximum site ratio of one dye molecule per three base pairs. It is not surprising that A-RNA (Arnott et al., 1973), conformationally distinct from B-DNA (Langridge et al., 1960), would impose different requirements for intercalative binding. The conformation of A-RNA (and all A-class double-stranded polynucleotides) is characterized by the C(3′)-endo puckering of the sugar rings while, in B-DNA, there is exclusively C(2′)-endo puckering. Crystal structures of several self-complementary dinucleoside monophosphates containing a bound intercalator have been reported (Tsai et al., 1975, 1977; Seeman et al., 1975; Jain et al., 1977; Sakore et al., 1977; Neidle et al., 1977), including a recent structure of $[(terpy)Pt(HET)]^+$ intercalated within the DNA fragment d(CpG) (Wang et al., 1978). These studies provide some information about the conformational distortions that must accompany dye binding to a polynucleotide. In all but one instance the sugar puckering of the dinucleoside phosphates at the intercalation site was found to be C(3′)-endo (3′,5′)-C(2′)-endo. This result has been used to rationalize the neighbor exclusion effects (Sobell et al., 1976, 1977). If this alternating mixed puckering mode is required for intercalative binding to the polymer, then, at most, every other interbase-pair site can be occupied at saturation. An exception to this trend was found in the crystal structure of the 3:2 complex of proflavine with CpG, which exhibits a normal RNA conformation with C(3′)-endo puckering (Neidle et al., 1977). Linked-atom molecular modeling of proflavin intercalation into B-DNA (Alden & Arnott, 1975) showed the mixed puckering mode to be stereochemically most favorable while, in contrast, a model where all sugars retain the characteristic C(3′)-endo puckering was found to be the optimum conformation for intercalative binding of proflavin to A-DNA and RNA (Alden & Arnott, 1977). It therefore is important to examine experimentally the influence of polymer conformation on the intercalation process.

Materials and Methods

Solutions were prepared by using distilled deionized water with glassware cleaned as described previously (Strothkamp & Lippard, 1976). Plastic pipet tips and ultracentrifuge tubes were cleaned with 5% HF, followed by exhaustive rinsing with deionized water.

Buffers and Chemicals. Experiments were carried out in buffer 1, 0.2 M sodium chloride and 0.05 M Tris-HCl, pH

[1] Abbreviations used: EtdBr, ethidium bromide; terpy, 2,2′,2″-terpyridine; HET, 2-hydroxyethanethiolate; py, pyridine; en, ethylenediamine; r_f, formal ratio of metal to nucleotide concentrations; r, ratio of bound metal to nucleotide concentrations; NMR, nuclear magnetic resonance; P_0, concentration of nucleotide.

7.5, or buffer 2, 1 mM sodium phosphate and 3 mM sodium chloride, pH 7.4. Ethidium bromide hemihydrate was purchased from the Sigma Chemical Co. Concentrations were determined spectrophotometrically by using $\epsilon_{285} = 54\,000$ (M cm)$^{-1}$ (Hsieh & Wang, 1975). The complex [(terpy)Pt(HET)]NO_3 was prepared as described elsewhere (Jennette et al., 1976). Tritiated [(terpy)Pt(HET)]$^+$, having a specific activity of approximately 38 mCi/mmol, was synthesized by using ^{3}H[(terpy)PtCl]Cl (Strothkamp & Lippard, 1976). The product was usually diluted with unlabeled [(terpy)Pt(HET)]$^+$ for binding studies. Bis(pyridine)ethylenediamineplatinum(II) perchlorate, $[(py)_2Pt(en)](ClO_4)_2$, was prepared according to the procedure of Appleton & Hall (1971). Concentrations were determined spectrophotometrically by using $\epsilon_{342\ nm}^{[(terpy)Pt(HET)]^+} = 12\,500$ (M cm)$^{-1}$ and $\epsilon_{266\ nm}^{[(py)_2Pt(en)]^{2+}} = 4150$ (M cm)$^{-1}$ (Gruskin, unpublished results). All spectral measurements of [(terpy)Pt(HET)]$^+$ were made within the range (<15 μM) where Beer's law applies.

Nucleic Acids. Calf thymus DNA (Type I) was purchased from the Sigma Chemical Co. and purified as described previously (Jennette et al., 1974). Poly(A), poly(U), and poly(I)·poly(C) were purchased from P-L Biochemicals. These polynucleotides were purified in the following manner. The polymer was extracted 2 or more times with freshly distilled phenol (equal volumes) which had previously been saturated with buffer 1 and neutralized with 1 N NaOH. The polymers were then precipitated twice with 2 volumes of 95% ethanol, redissolved in buffer 1 containing 0.01 M ethylenediaminetetraacetate (EDTA), and dialyzed extensively into the appropriate buffer. Poly(A)·poly(U) was formed from its constituent strands by combining the homopolymers in equimolar proportions and extensively dialyzing for at least 24 h. Concentrations were determined spectrophotometrically by assuming the following molar extinction coefficients: $\epsilon_{A\cdot U}(260\ nm) = 7140$ (M cm)$^{-1}$ (Schmechel & Crothers, 1971) and $\epsilon_{I\cdot C}(260\ nm) = 5000$ (M cm)$^{-1}$ (Chamberlin & Patterson, 1965). These synthetic polymers were characterized by their melting transitions in buffer 1: T_m(A·U) = 65.3 °C, percent hypochromicity = 57; T_m(I·C) = 64.5 °C, percent hypochromicity = 42.

Apparatus. Spectrophotometric measurements were made with a Cary 118C recording spectrophotometer. In thermal denaturation experiments, the temperature in the cuvette was monitored with an iron–constantan thermocouple and a Leads and Northrup potentiometer. Pelleting experiments were performed with a Beckman Model L4-50 preparative ultracentrifuge. Radioactivity was measured by using a Searle Analytic Isocap/300 ambient temperature liquid scintillation counter. Wheaton vials made of Vitro "180" low-potassium glass were employed and Bray's scintillation mixture was used throughout (Bray, 1960). Data analysis was performed by using an IBM 360-91 computer. Viscosity measurements were carried out at 25 °C by using a Zimm-Crothers low-shear viscometer (Spinco Division of Beckman Instruments, Inc.).

Viscosity Studies. All solutions were passed through 0.45-μm Millipore filters prior to mixing. Molecular weights of the duplex RNAs used were estimated (Crothers & Zimm, 1965) through viscosity measurements to be in the range of 500 000–800 000. The RNA concentration, P_0, was kept constant at 5×10^{-4} mol of nucleotide per L. Intrinsic viscosities, $[\eta]$, were calculated from reduced viscosities, η_{sp}/P_0, with the use of the estimate of 0.5 for Huggin's coefficient, k in eq 1 (Cohen & Eisenberg, 1969; Huggins, 1942).

$$\frac{\eta_{sp}}{P_0} = [\eta](1 + k[\eta]P_0) \qquad (1)$$

Corrections to the reduced viscosity ratios, at various concentrations of bound dye, did not exceed 2%. Length increases were approximated from the intrinsic viscosity ratios by using eq 2 derived (Schmechel & Crothers, 1971) for ellipsoids of

$$\frac{L_r}{L_0} = \left(\frac{[\eta]_r}{[\eta]_0}\right)^{0.356}\left(\frac{b_0}{b_r}\right)^{0.0677} \qquad (2)$$

revolution, where L_0 is the length of polymer in the absence of dye and L_r is the length of polymer in the presence of dye at a particular value of r, the ratio of bound dye to nucleotide concentration. Calculated lengths were not corrected for variation in the minor axis, b, of the polymer ellipsoid on dye binding.

Binding isotherms were obtained through pelleting experiments at 20 °C in the ultracentrifuge in the following manner. Concentrated polynucleotide solutions were prepelleted at 192000g for at least 17 h, and the supernatant was discarded. The pellets were then redissolved in buffer, and 1-mL aliquots were mixed with 5-mL portions of stock solutions of varying dye concentrations. The dye–polymer solution was then centrifuged at 192000g for at least 1.5 h longer than the prepellet in order to ensure that all the polynucleotide would sediment. Supernatants were decanted, and the free-dye concentrations were measured spectrophotometrically (for EtdBr) or by liquid scintillation counting (for [^{3}H][(terpy)Pt(HET)]$^+$). Polyallomar tubes were used for ultracentrifugation, as cellulose nitrate tubes were found to bind [(terpy)Pt(HET)]$^+$ weakly. For [(terpy)Pt(HET)]$^+$ experiments, specific activity curves were obtained by counting aliquots of the platinum stock solutions, the concentrations of which had been measured spectrophotometrically. Initial dye concentrations in dye–polymer solutions were determined by counting aliquots and/or computations based on the dilution of stock dye solutions. Studies performed with ^{3}H[(terpy)Pt(HET)]$^+$, measured by its radioactivity, and [(terpy)Pt(HET)]$^+$ (unlabeled), measured spectrophotometrically, were found to agree within experimental error. In previous work (Jennette et al., 1976), [(terpy)Pt(HET)]$^+$ was found to have a dimerization constant, K_D, of 7 (±5) × 10^3 M^{-1}. Accordingly, all data have been corrected for the dimerization of free dye in solution, eq 3, where C_M is the concentration

$$C_M = \frac{-1 + \sqrt{1 + 8K_DC_F}}{4K_D} \qquad (3)$$

of free monomer in solution and C_F is the total concentration of free dye in solution. The large error associated with the value of K_D produces a 10% maximum uncertainity in monomer concentration (C_M) over the total dye concentrations used in the pelleting experiments. Solutions containing [(terpy)Pt(HET)]$^+$ and poly(A)·poly(U) at concentrations employed in the binding studies were also centrifuged at low speed for short times (20000g for 1 h) and, additionally, examined in the analytical ultracentrifuge to assay for precipitation. For $r > 0.30$, ~10% precipitation was found although none was observed at lower r values. After 24-h incubations at room temperature, however, appreciable precipitation (~30%) was observed which may reflect aggregation of the polynucleotides.

Binding isotherms are compared with those derived from a general statistical mechanical model that describes the binding of small molecules to a one-dimensional lattice of equivalent interbase-pair sites. The binding is characterized by the following parameters: (1) the intrinsic binding constant, $K(0) = \exp(-\Delta G°/RT)$, where $\Delta G°$ = standard free energy in binding to an individual site; (2) the degree of exclusion,

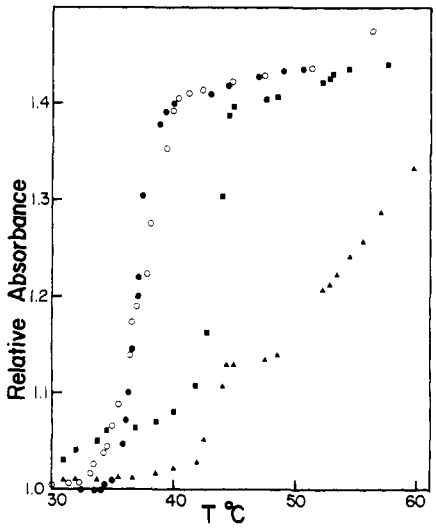

FIGURE 2: Thermal denaturation of poly(A)·poly(U) in buffer 2 in the presence of (■) $[(terpy)Pt(HET)]^+$, Pt_{tot} = 4.6 μM, P_0 = 35 μM, and (●) $[(py)_2Pt(en)]^{2+}$, Pt_{tot} = 15 μM, P_0 = 42 μM, and in the absence (○) of platinum complexes, P_0 = 68 μM, where the absorbance is monitored at 260 nm. Also, the denaturation profile of poly(A)·poly(U) in the presence of $[(terpy)Pt(HET)]^+$ monitored at 342 nm (▲) is indicated.

l, defined as the minimum number of base pairs that separates two bound dye molecules; and (3) the cooperativity factor, $\tau = \exp(-\Delta G^\circ(l)/RT)$, where $\Delta G^\circ(l)$ is the additional free energy of binding of a dye molecule in the presence of a second dye l base pairs away. The equations (4 and 5)

$$r = \frac{1}{2}\frac{[(\tau - 1)y^2 + (1 - 2\tau)y + \tau]}{[(l\tau - l)y^2 + (1 + l - 2l\tau)y + l\tau]} \quad (4)$$

$$K(0)C = \frac{(1 - y)}{(l - \tau)y^{l+1} + y^l\tau} \quad (5)$$

governing this binding have been derived by Bresloff and Crothers (Bresloff, 1974). The variables are r, the ratio of bound dye to nucleotide concentrations, C, the concentration of free monomer dye in solution, and y, a statistical weighting factor. By applying these equations to the results of the binding experiments, one can determine the degree of anticooperativity, given by l (l = 2 for nearest-neighboring site exclusion), the degree of cooperativity, given by τ (τ = 1 for random distribution subject only to exclusion constraints), and the intrinsic binding constant, $K(0)$. These three parameters are the chief characteristics of a particular dye–polynucleotide interaction. The pelleting data were fit to eq 4 and 5 by using an iterative, nonlinear least-squares analysis computer program where both $K(0)$ and τ are varied simultaneously for a given integer value of l. An alternative but analogous set of equations has been derived and applied to the cooperative interactions of proteins with nucleic acids (McGhee & von Hippel, 1974).

Results

Thermal Denaturation of Poly(A)·Poly(U). The effect of $[(terpy)Pt(HET)]^+$ on the melting temperature (T_M) of poly(A)·poly(U) in buffer 2 is shown in Figure 2. Changes in absorbance were monitored at both 260 nm, reflecting the RNA hypochromicity, and, in the presence of $[(terpy)Pt(HET)]^+$, at 342 nm, reflecting the hypochromicity of the dye molecule. Previous work (Strothkamp & Lippard, 1976; Jennette et al., 1976) suggests that the 342-nm band is characteristic of sulfur binding to the fourth coordination site in platinum terpyridine complexes. By use of A_{260} to monitor the transition, T_M is found to increase from 37 to 43 °C in the presence of $[(terpy)Pt(HET)]^+$ at a formal ratio (r_f) of dye to nucleotide concentrations of 0.13. This result indicates that the duplex structure has been stabilized. The 342-nm band shows two hypochromic changes. The first of these parallels that at 260 nm and is associated with the melting of this helix. At higher temperatures a second, broad transition occurs. If the platinum intercalators were stacked to some extent with the bases of the single-stranded polynucleotide, the second, broad transition might correspond to the melting out of this secondary interaction. Decomposition of the platinum complex accompanied by covalent binding of the $[(terpy)Pt]^{2+}$ moiety to the bases does not occur. The absorbance at 342 nm fully increases to that of free $[(terpy)Pt(HET)]^+$, and the 350–300-nm region of the spectrum at high temperature matches that of free $[(terpy)Pt(HET)]^+$.

A significant increase in the melting temperature of poly(A)·poly(U) is not observed (Figure 2) in the presence of $[(py)_2Pt(en)]^{2+}$. This platinum complex was found (Lippard et al., 1976) not to intercalate into DNA. Here the pyridine rings are expected to rotate out of the coordination plane of the molecule. A 90° rotation of the pyridine rings out of the coordination plane is observed in crystal structures (Mason & Towl, 1970; Doedens & Dahl, 1966; Dobinson et al., 1967) of a variety of *cis*-bis(pyridine)–metal complexes having either octahedral or square-planar geometries. The electrostatic interactions between the $[(py)_2Pt(en)]^{2+}$ dication and the polynucleotide are not sufficient to stabilize a duplex rather than a random-coil polymer structure.

A 2 °C increase in the T_M of poly(A)·poly(U) in the presence of $[(terpy)Pt(HET)]^+$ at an r_f of 0.08 was observed in buffer 1, where high temperatures are necessary to monitor the complete transition.

Control Studies. Optical studies of the $[(terpy)Pt(HET)]^+$–poly(A)·poly(U) complex were carried out in buffer 1 to ascertain whether, under the conditions of the pelleting experiments, disruption of the polymer duplex by some process other than intercalation might occur. Possibilities include covalent binding, degradation of the polynucleotide, or formation of triple-stranded helixes. The optical spectrum of a $[(terpy)Pt(HET)]^+$–poly(A)·poly(U) solution at ambient temperature was monitored for a period of 48 h, the maximum time used for a pelleting experiment. A change in the 300–350-nm spectral region would be expected to accompany slow covalent binding. No change in the UV spectrum was observed. Supernatants from pelleting experiments were monitored spectrophotometrically to test for possible RNA degradation. The UV spectrum corresponds to that of $[(terpy)Pt(HET)]^+$ in the absence of nucleotides. No increase in A_{260} was observed. The spectrum of the $[(terpy)Pt(HET)]^+$–polymer solution in buffer 1 was examined before and after thermal denaturation. A hyperchromic change at 280 nm has been shown (Stevens & Felsenfeld, 1964) to accompany the formation of triple-stranded helixes. No change in absorbance at 280 nm was observed on heat denaturation of the solution, indicating that the presence of $[(terpy)Pt(HET)]^+$ does not facilitate formation of poly(A)·2[poly(U)] in buffer 1.

Viscosity Measurements. Both $[(terpy)Pt(HET)]^+$ and EtdBr increase the viscosity of poly(A)·poly(U) at low r values. As shown in Figure 3a, the specific viscosity of the RNA solution increases with increasing concentration of bound $[(terpy)Pt(HET)]^+$ and EtdBr. Saturation values for platinum binding could not be investigated through viscosity measurements since, at the high poly(A)·poly(U) concentrations

Table I: Summary of Intercalation Binding Parameters in Buffer 1 at 20 °C[a]

dye	polynucleotide	eq	r_{max}	$K(0)$	τ	l
EtdBr	calf thymus DNA	4, 5	0.25	2.1(2) × 10^5 M^{-1}	1.0(2)	2
[(terpy)Pt(HET)]$^+$	calf thymus DNA	4, 5	0.25	1.6(1) × 10^4 M^{-1}	1.5(2)	2
EtdBr	poly(A)·poly(U)	4, 5	0.167	3.5(5) × 10^5 M^{-1}	6(1)	3
[(terpy)Pt(HET)]$^+$	poly(A)·poly(U)	7, 8	0.333	1.2(1) × 10^9 M^{-2}	4.8(2)	3
[(terpy)Pt(HET)]$^+$	poly(I)·poly(C)	7, 8	0.333	8.4(8) × 10^7 M^{-2}	6.6(4)	3

[a] Parameters used are defined in the text. Standard deviations are given in parentheses and refer to the least significant digit. The value of $[K(0)]^{1/2}$ provides the average value of the binding constant per mole of bound dye for the [(terpy)Pt(HET)]$^+$–RNA interactions.

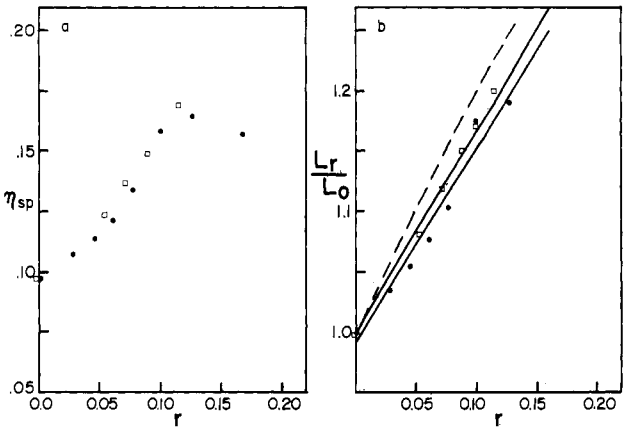

FIGURE 3: (a) Specific viscosity of poly(A)·poly(U) at 25 °C as a function of the bound concentrations of [(terpy)Pt(HET)]$^+$ (●) and EtdBr (□) in buffer 1. The r values have been computed from the binding parameters in Table I. $C_{A\text{-}U}$ = 4.65 × 10^{-4} M; Pt concentrations ranged from 0 to 70 μM. EtdBr concentrations ranged from 0 to 53 μM. (b) Length increases calculated for [(terpy)Pt(HET)]$^+$ (●) and EtdBr (□) intercalation based on viscosity measurements. The dashed line indicates the theoretical limit for 100% intercalation, an increase of one base-pair thickness per intercalated dye.

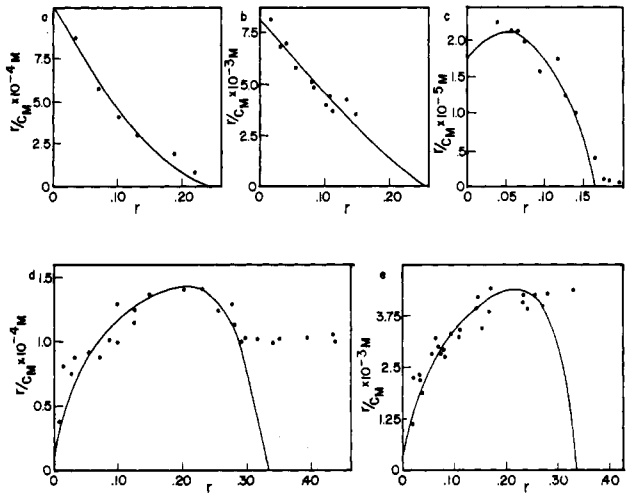

FIGURE 4: Scatchard plots of dyes bound to polynucleotides, obtained by the pelleting method, in buffer 1 at 20 °C. Binding curves were determined by fitting the data to eq 4 and 5 for a, b, and c and eq 7 and 8 for d and e. Dye concentrations were varied from 5 to 200 μM with polymer concentrations of 50–100 μM. (a) EtdBr + calf thymus DNA; (b) [(terpy)Pt(HET)]$^+$ + calf thymus DNA; (c) EtdBr + poly(A)·poly(U); (d) [(terpy)Pt(HET)]$^+$ + poly(A)·poly(U); (e) [(terpy)Pt(HET)]$^+$ + poly(I)·poly(C).

necessary for this experiment, precipitation of the dye–polymer complex occurred at $r_{Pt} \geq 0.20$. Approximate length increases were calculated from the viscosity data by using eq 2. As shown in Figure 3b, the plot of L_r/L_0 vs. r is linear. Calculations of the length increase have assumed the polymer to behave like an ellipsoidal rod at the molecular weight range employed, where contributions to the viscosity increase owing to chain stiffening are small. Also, only length ratios have been considered. The dependence of the length increase on the concentration of bound dye may be given by eq 6 (Schmechel

$$\frac{L_r}{L_0} = 1 + \alpha r \qquad (6)$$

& Crothers, 1971). For the case where the polymer chain increases in length by one base-pair spacing per intercalated dye, α equals 2.0. This value of α may be compared to those of poly(A)·poly(U) in the presence of [(terpy)Pt(HET)]$^+$ and EtdBr, 1.64 and 1.73, respectively.

Pelleting Experiments. Results of the pelleting experiment are shown in Scatchard plot form (Scatchard, 1949) in Figure 4. The binding parameters are summarized in Table I. As a test of the validity of the pelleting method, the binding isotherm of EtdBr with calf thymus DNA was determined. The Scatchard plot (Figure 4a) shows the characteristic curvature of the binding of intercalators to naturally occurring DNAs. EtdBr binds to calf thymus DNA in a nearest-neighbor excluded fashion, l = 2. No cooperativity in its binding is observed, τ = 1. Conventional analysis (Jennette et al., 1974) of the data gave an apparent binding constant (K_{app}), computed as the slope of the r/C_M vs. r plot, of 3.9 × 10^5 M^{-1}. A literature value (LePecq & Paoletti, 1967) for the apparent binding constant of EtdBr to calf thymus DNA, extrapolated to the same ionic strength as buffer 1, is 3.4 × 10^5 M^{-1} at 23 °C.

The complex [(terpy)Pt(HET)]$^+$ binds to calf thymus DNA in a similar fashion, as shown in Figure 4b. No significant degree of cooperativity (τ = 1.5) is associated with the nearest-neighbor excluded (l = 2) binding. As reflected in the intrinsic binding constants, $K(0)$, the affinity of [(terpy)Pt(HET)]$^+$ for calf thymus DNA is less than that of EtdBr.

The characteristics of EtdBr binding to poly(A)·poly(U) (Figure 4c) differ from those observed in binding either dye molecule to calf thymus DNA. The best fit to eq 4 and 5 gives a value of l = 3 for the degree of anticooperativity, implying a saturation binding of one ethidium to a site encompassing three base pairs. Moreover, the degree of cooperativity is increased; data analysis gives a τ value of 6. Bresloff (Bresloff, 1974) has determined that l = 3 and τ = 2.3 for EtdBr binding to poly(A)·poly(U) in 1 M salt. An increased cooperativity of binding occurs in 0.2 M NaCl.

The binding isotherms of [(terpy)Pt(HET)]$^+$ with poly(A)·poly(U) and poly(I)·poly(C) are shown in Figure 4d and 4e, respectively. The complex [(terpy)Pt(HET)]$^+$ binds to these polynucleotides in a highly cooperative fashion; the Scatchard plots of the data show large positive curvature. Analysis of this data required that further constraints be placed on the general binding model given by eq 4 and 5. In particular, the poly(A)·poly(U)–[(terpy)Pt(HET)]$^+$ binding data suggest that at saturation two platinum molecules are bound in a three-base-pair site, r_{max} = 0.333. The poly(I)·poly(C)–[(terpy)Pt(HET)]$^+$ binding isotherm, showing a large degree of cooperativity and very low binding affinity, does not reveal the saturation dye/phosphate ratio. At high binding

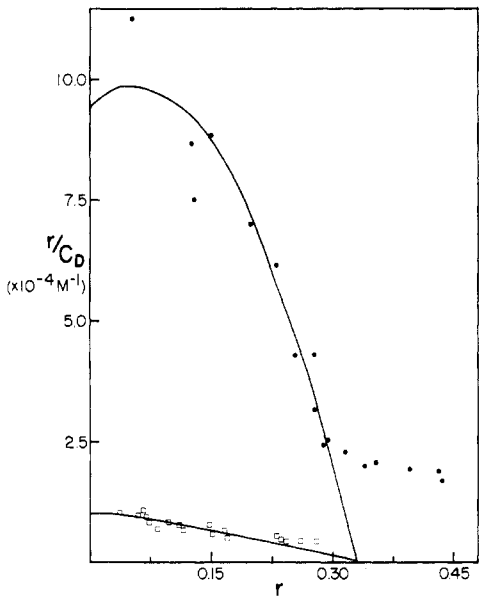

FIGURE 5: Replot of data in Figure 4d and 4e based on binding of $[(terpy)Pt(HET)]^+$ to the polynucleotides in equilibrium with platinum dimers. In this plot closed circles represent the binding of $[(terpy)Pt(HET)]^+$ with poly(A)·poly(U) and open squares represent the binding of $[(terpy)Pt(HET)]^+$ with poly(I)·poly(C). Low-concentration data ($C_D < 2$ μM) have been omitted owing to uncertainty in the dimerization constant.

ratios, some precipitation of the dye–polymer complex was observed.

Cooperativity may be built into the general binding model by constraining the platinum molecules to occupy sites along the backbone in pairs only. The pelleting data for $[(terpy)Pt(HET)]^+$ binding to RNA were therefore fit to the equations

$$r = \frac{(\tau - 1)y^2 + (1 - 2\tau)y + \tau}{(3\tau - 3)y^2 + (4 - 6\tau)y + 3\tau} \quad (7)$$

$$K(0)C_M^2 = \frac{(1 - y)}{(1 - \tau)y^4 + y^3\tau} \quad (8)$$

where the pair of dye molecules are bound to a three-base-pair site, $l = 3$. Here $K(0)$ reflects the binding of a pair of platinum molecules to an individual three-base-pair site, and τ reflects the cooperativity associated with this repeating unit. An average value of the binding constant per dye bound may be obtained as the square root of $K(0)$, 3.5×10^4 M^{-1} for poly(A)·poly(U) with $[(terpy)Pt(HET)]^+$. This value is 1 order of magnitude lower than that found for the binding of EtdBr to poly(A)·poly(U). The pelleting data agree favorably with this binding model.

The platinum–RNA binding data may also be presented as a plot of r/C_{dimer} vs. r, as shown in Figure 5. The solid lines were constructed by fitting the data to eq 4 and 5, where C is now given by the concentration of free dimer in solution. This analysis corresponds to a model where only dimeric $[(terpy)Pt(HET)]^+$ units bind to the polymer. In fact, this treatment of the data is mathematically analogous to that of eq 7 and 8. The plots clearly show a saturation point corresponding to two platinum molecules bound to a site encompassing three base pairs.

Discussion

Studies of the equilibrium binding of $[(terpy)Pt(HET)]^+$ to poly(A)·poly(U) are consistent with an intercalative mode of interaction. The complex $[(terpy)Pt(HET)]^+$ increases the melting temperature of poly(A)·poly(U). This stabilization of a helical rather than a random-coiled form of the RNA by the bound dye is expected for intercalation. Covalent bonding of the terpyridine–platinum complex to either the bases or to the phosphate backbone does not occur. The substitutionally inert platinum–sulfur bond remains intact over the course of all experiments as monitored through its optical spectrum. Electrostatic interactions, for example, on the outside of the RNA, are insufficient to produce the duplex structure stabilization observed. The nonintercalating $[(py)_2Pt(en)]^{2+}$ dication does not produce an increase in the polymer melting temperature. The presence of the cationic metal complex does not facilitate the formation of a triple-stranded helix. The optical changes accompanying the denaturation of poly(A)·poly(U) are not observed on denaturing the polynucleotide complex in the presence of $[(terpy)Pt(HET)]^+$ under the buffer conditions of the pelleting experiment. In addition, comparable binding isotherms are observed for both poly(A)·poly(U) and poly(I)·poly(C). The latter has been found not to disproportionate into a triple-stranded helix under a variety of conditions investigated (Chamberlin & Patterson, 1965). Hydrodynamic measurements provided indirect evidence for RNA lengthening on binding of $[(terpy)Pt(HET)]^+$. The linear increase L_r/L_0 with r on binding of both $[(terpy)Pt(HET)]^+$ and EtdBr is consistent with intercalation, and reasonable agreement is obtained between the expected length increase on intercalation and the observed length increase as estimated through viscosity measurements.

The ultracentrifugation pelleting method was found to give reproducible binding data through direct measurement of the free-dye concentration. Other laboratories (Pohl et al., 1972; Hsieh & Wang, 1975; Lloyd et al., 1968) have employed a comparable procedure where, by using an analytical ultracentrifuge, the separation between bound and free dye is observed during the course of the polymer sedimentation. Equilibrium dialysis, a more common method of assaying dye binding, proved unsuccessful owing to strong binding of the dye, as well as dye–polymer complex, to the dialysis membrane. Binding data for EtdBr with calf thymus DNA obtained through the pelleting method agree closely with data obtained through other experimental procedures (LePecq & Paoletti, 1967).

The binding isotherm determined through pelleting experiments reflects strong cooperativity in the interaction of $[(terpy)Pt(HET)]^+$ with poly(A)·poly(U). The large positive curvature in the Scatchard plot implies stabilization of the polynucleotide structure by long runs of successively bound dye. The data suggest the equilibrium binding of dye in pairs, the binding of one dye molecule strongly facilitating occupation of a neighboring site. A model in which such pairs of dye molecules bind to the RNA nicely accounts for the experimental isotherm. This same cooperativity is observed in the poly(I)·poly(C)–$[(terpy)Pt(HET)]^+$ Scatchard plot. It may also be seen that at high r values, even above the supposed saturation maximum, the r/C_M curve is significantly above zero. This result is ascribed to precipitation of the complex when the charge on the polynucleotide has been neutralized owing either to cooperative intercalative binding or to stacking of the cationic dye molecules on the outside of the helical polyanion.

The binding characteristics of $[(terpy)Pt(HET)]^+$ and EtdBr with DNAs are very similar. The spatial similarity of these two molecules is illustrated in Figure 1. The Scatchard plots of Figure 4a and 4b compare closely in their curvature, the isotherms differing only because the magnitudes of the intrinsic

binding constants are unequal (Table I). Differences in the binding of ethidium and [(terpy)Pt(HET)]$^+$ to poly(A)·poly(U) are quite clearly seen by comparing Figure 4c and 4d. Intercalation models for these two dyes bound to poly(A)·poly(U) reveal that, at saturation, one ethidium cation is bound to a site encompassing three base pairs while two [(terpy)Pt(HET)]$^+$ molecules bind cooperatively to the same three-base-pair site. Both [(terpy)Pt(HET)]$^+$ and EtdBr dimerize in the solution. The dimerization constant of [(terpy)Pt(HET)]$^+$ (Jennette et al., 1976), however, is substantially higher than that of ethidium (Pulleybank & Morgan, 1975). It is interesting that only in the crystal structure where proflavin is bound to CpG does the C(3′)-endo puckering of both sugars occur (Neidle et al., 1977). Proflavin, like [(terpy)Pt(HET)]$^+$, is characterized by a relatively large dimerization constant (Schwartz et al., 1970). The features contributing to the ability of [(terpy)Pt(HET)]$^+$ to self-associate may also govern the cooperative stacking interaction exhibited in its binding to poly(A)·poly(U). Perhaps intercalators that form stable dimers bind RNA with exclusively C(3′)-endo puckering at the intercalation site while mixed-mode puckering occurs in the RNA binding of intercalators that do not strongly self-associate. This idea is consistent with the crystal structures of intercalated RNA fragments that have been determined thus far and could be further tested, for example, by an X-ray structure determination of [(terpy)-Pt(HET)]$^+$ cocrystallized with CpG. In addition, the hydroxyethyl tail of [(terpy)Pt(HET)]$^+$ may hydrogen bond to the phosphate backbone or to the 2′-hydroxyl oxygen of the ribose, stabilizing a specific poly(A)·poly(U) interaction. Structurally different hydrogen-bonding possibilities exist for the amino groups of the ethidium cation, although X-ray diffraction results for dinucleoside monophosphates suggest that intercalated ethidium may not be involved in hydrogen bonding (Tsai et al., 1975).

Studies with both intercalation reagents reflect substantial differences in their binding to poly(A)·poly(U) and naturally occurring DNAs (Table I). EtdBr and [(terpy)Pt(HET)]$^+$ have been shown in a variety of investigations (LePecq & Paoletti, 1967; Bond et al., 1975; Bresloff, 1974; Crothers, personal communication) to bind to DNAs according to the nearest-neighbor-exclusion constraints. Although it has been found that an increase in the cooperativity of ethidium binding is associated with binding to synthetic DNAs of repeating sequence, the interactions of [(terpy)Pt(HET)]$^+$ and ethidium with DNAs are strictly governed by the neighbor-exclusion principle. Our results, consistent with those of Bresloff and Crothers (Bresloff, 1974; Crothers, personal communication), indicate that the exclusion extends to two base pairs on binding ethidium to duplex RNA. The reason for this exclusion is unclear. The complex [(terpy)Pt(HET)]$^+$ also exhibits striking differences in its binding to natural DNAs and poly(A)·poly(U). The binding of [(terpy)Pt(HET)]$^+$ to poly(I)·poly(C) and poly(A)·poly(U) are similar, differing only in binding constant. Since both synthetic polymers are conformationally analogous to naturally occurring duplex RNAs (Arnott et al., 1973), these results may reflect the general RNA binding behavior of [(terpy)Pt(HET)]$^+$. In particular, [(terpy)Pt-(HET)]$^+$ binds duplex RNA under constraints differing substantially from those imposed by the structure of DNA. Maintenance of C(3′)-endo puckering along the RNA polymer, as stereochemical modeling suggests (Alden & Arnott, 1977), would allow an increased binding level over the neighbor-excluded limit found in DNA, where mixed sugar puckering appears to dominate (Alden & Arnott, 1975). Particular features of [(terpy)Pt(HET)]$^+$, i.e., its high dimerization constant and the hydrogen-bonding capability of its hydroxyethyl tail, and the conformational constraints of double-stranded RNA, having C(3′)-endo puckering and the 2′-hydroxyl group positioned toward the intercalation site, may combine to produce the distinctive, cooperative binding mode that is observed. The cooperativity observed in the intercalation of [(terpy)Pt(HET)]$^+$ into poly(A)·poly(U) is, furthermore, likely to be enhanced by the repetitive nature of the secondary structure projected along the helix of this synthetic polynucleotide.

The present results reveal the ability of intercalators to distinguish regions of differing secondary structure. Detailed studies of protein–substrate interactions have uncovered conformational requirements for site recognition. The conformational influence of the polynucleotide on the binding of [(terpy)Pt(HET)]$^+$ to DNAs and RNAs may reflect the ability of intercalating drugs to recognize differences in nucleic acid structure. It is tempting to suggest that rRNA and tRNA, possessing regions of A-RNA conformation, may serve as templates for specific drug recognition.

Acknowledgments

We thank J. Lehmann for excellent technical assistance.

References

Aktipis, S., & Martz, W. W. (1974) *Biochemistry 13*, 112.
Alden, C. J., & Arnott, S. (1975) *Nucleic Acids Res. 2*, 1701.
Alden, C. J., & Arnott, S. (1977) *Nucleic Acids Res. 4*, 3855.
Appleton, T. G., & Hall, J. R. (1971) *Inorg. Chem. 10*, 1717.
Arnott, S., Hukins, D. W. L., Dover, S. D., Fuller, W., & Hodgson, A. R. (1973) *J. Mol. Biol. 81*, 107.
Ballesta, J. P. G., Waring, M. J., & Vasquez, D. (1976) *Nucleic Acids Res. 3*, 1307.
Bond, P. J., Langridge, R., Jennette, K. W., & Lippard, S. J. (1975) *Proc. Natl. Acad. Sci. U.S.A. 72*, 4825.
Bray, G. A. (1960) *Anal. Biochem. 49*, 343.
Bresloff, J. (1974) Ph.D. Dissertation, Yale University, New Haven, CT.
Cairns, J. (1962) *Cold Spring Harbor Symp. Quant. Biol. 27*, 311.
Chamberlin, M. J., & Patterson, D. L. (1965) *J. Mol. Biol. 12*, 410.
Cohen, G., & Eisenberg, H. (1969) *Biopolymers 8*, 45.
Crothers, D. M. (1968) *Biopolymers 6*, 575.
Crothers, D. M., & Zimm, B. H. (1965) *J. Mol. Biol. 12*, 525.
Dobinson, G. C., Mason, R., & Russell, D. R. (1967) *Chem. Commun.*, 62.
Doedens, R. J., & Dahl, L. F. (1966) *J. Am. Chem. Soc. 88*, 4847.
Douthart, R. J., Burnett, J. P., Beasbey, F. W., & Frank, B. H. (1973) *Biochemistry 12*, 214.
Heitner, H. I., Lippard, S. J., & Sunshine, H. R. (1972) *J. Am. Chem. Soc. 94*, 8936.
Howe-Grant, M., Wu, K. C., Bauer, W. R., & Lippard, S. J. (1976) *Biochemistry 15*, 4339.
Hsieh, J., & Wang, J. C. (1975) *Biochemistry 14*, 527.
Huggins, M. L. (1942) *J. Am. Chem. Soc. 64*, 2716.
Jain, S. C., Tsai, C.-C., & Sobell, H. M. (1977) *J. Mol. Biol. 114*, 317.
Jennette, K. W. (1975) Ph.D. Dissertation, Columbia University, New York.
Jennette, K. W., Lippard, S. J., Vassiliades, G. A., & Bauer, W. R. (1974) *Proc. Natl. Acad. Sci. U.S.A. 71*, 3839.
Jennette, K. W., Gill, J. T., Sadownick, J. A., & Lippard, S. J. (1976) *J. Am. Chem. Soc. 98*, 6159.

Jones, C. R., Kearns, D. R., & Muench, K. H. (1976) *J. Mol Biol. 103*, 747.
Kearns, D. R., & Jones, C. R. (1975) *Biochemistry 14*, 2660.
Langridge, R., Wilson, H. R., Hooper, C. W., Wilkins, M. H. F., & Hamilton, L. D. (1960) *J. Mol. Biol. 2*, 19.
LePecq, J. B., & Paoletti, C. (1967) *J. Mol. Biol. 27*, 87.
Lerman, L. S. (1961) *J. Mol. Biol. 3*, 18.
Liebman, M., Rubin, J., & Sundaralingam, M. (1977) *Proc. Natl. Acad. Sci. U.S.A. 74*, 4821.
Lippard, S. J., Bond, P. J., Wu, K. C., & Bauer, W. R. (1976) *Science 194*, 726.
Lloyd, P. H., Prutton, R. N., & Peacock, A. R. (1968) *Biochem. J. 107*, 353.
Mason, R., & Towl, A. D. C. (1970) *J. Chem. Soc. 9*, 1601.
McGhee, J. D., & von Hippel, P. H. (1974) *J. Mol. Biol. 86*, 469.
Neidle, S., Achari, A., Taylor, G. L., Berman, H. M., Carell, H. L., Glusker, J. P., & Stallings, W. C. (1977) *Nature (London) 269*, 304.
Pohl, F. M., Jovin, T. M., Baehr, W., & Holbrook, J. J. (1972) *Proc. Natl. Acad. Sci. U.S.A. 69*, 3805.
Pulleybank, D. E., & Morgan, A. R. (1975) *J. Mol. Biol. 91*, 1.
Sakore, T. D., Jain, S. C., Tsai, C.-C., & Sobell, H. M. (1977) *Proc. Natl. Acad. Sci. U.S.A. 74*, 188.
Scatchard, G. (1949) *Ann. N.Y. Acad. Sci. 51*, 660.
Schmechel, D. E. V., & Crothers, D. M. (1971) *Biopolymers 10*, 465.
Schwartz, G., Klose, S., & Balthasar, W. (1970) *Eur. J. Biochem. 12*, 454.
Seeman, N. C., Day, R. O., & Rich, A. (1975) *Nature (London) 253*, 324.
Sobell, H. M., Tsai, C.-C., Gilbert, S. G., Jain, S. C., & Sakore, T. D. (1976) *Proc. Natl. Acad. Sci. U.S.A. 73*, 3068.
Sobell, H. M., Tsai, C.-C., Jain, S. C., & Gilbert, S. G. (1977) *J. Mol. Biol. 114*, 333.
Stevens, C. L., & Felsenfeld, G. (1964) *Biopolymers 2*, 293.
Strothkamp, K. G., & Lippard, S. J. (1976) *Proc. Natl. Acad. Sci. U.S.A. 73*, 2536.
Sunshine, H. R., & Lippard, S. J. (1974) *Nucleic Acids Res. 1*, 673.
Tsai, C.-C., Jain, S. C., & Sobell, H. M. (1975) *Proc. Natl. Acad. Sci. U.S.A. 72*, 628.
Tsai, C.-C., Jain, S. C., & Sobell, H. M. (1977) *J. Mol. Biol. 114*, 301.
Wang, A. H. J., Nathans, J., van der Marel, G., van Boom, J. H., & Rich, A. (1978) *Nature (London) 276*, 471.
Waring, M. J. (1961) *Biochim. Biophys. Acta 114*, 234.
Wells, B. D., & Cantor, C. R. (1977) *Nucleic Acids Res. 4*, 1667.
Zama, M., & Ichimura, S. (1976) *Biopolymers 15*, 1693.

Kinetics and Mechanism of the Reduction of Horse Heart Ferricytochrome *c* by Glutathione†

Johannes Everse* and Nikola Kujundzic‡

ABSTRACT: A detailed investigation of the reduction of cytochrome *c* by glutathione has shown that the reaction proceeds through several steps. A rapid combination of the reducing agent with the cytochrome leads to the formation of a glutathione–cytochrome intermediate in which the glutathione most likely interacts with the edge of the heme moiety. The electron transfer takes place in a subsequent slower step. Since cytochrome *c*(III) exists in two conformational forms at neutral pH [Kujundzic, N., & Everse, J. (1978) *Biochem. Biophys. Res. Commun. 82*, 1211], the reduction of cytochrome *c* by glutathione may be represented by

$$\text{cyt } c(\text{III}) + \text{GS}^- \underset{}{\overset{K_1}{\rightleftharpoons}} \text{cyt } c(\text{III}) \ldots \text{GS}^- \xrightarrow{k_1} \text{products}$$

$$\text{cyt } c^*(\text{III}) + \text{GS}^- \underset{}{\overset{K_2}{\rightleftharpoons}} \text{cyt } c^*(\text{III}) \ldots \text{GS}^- \xrightarrow{k_2} \text{products}$$

At 25 °C, pH 7.5, and an ionic strength of 1.0 (NaCl), $k_1 = 1.2 \times 10^{-3}$ s^{-1}, $k_2 = 2.0 \times 10^{-3}$ s^{-1}, $K_1 = 2.9 \times 10^3$ M^{-1}, and $K_2 = 5.3 \times 10^3$ M^{-1}. The reaction is catalyzed by trisulfides, and second-order rate constants of 4.55×10^3 and 7.14×10^3 M^{-1} s^{-1} were obtained for methyl trisulfide and cysteine trisulfide, respectively.

Several years ago Dickerson et al. (1971) and Takano et al. (1973) elucidated the spatial structure of both the ferri- and ferrocytochrome *c* by X-ray diffraction. According to these studies, the heme group lies in a crevice of globular protein and is covalently bound to the protein by thioether bridges formed between the porphyrin ring and two cysteine residues in the peptide chain. The iron atom is positioned in the plane of the porphyrin ring with the fifth and sixth coordination sites occupied by a ring nitrogen atom of histidine-18 and the sulfur atom of methionine-80, respectively. An important feature of the structure is that one edge of the porphyrin ring is exposed to the surface of the protein.

A broad spectrum of oxidizing and reducing agents has been used to probe the reactivity of cytochrome *c* in the hope that its behavior in such reactions might advance our understanding of its function in vivo. Several detailed proposals regarding

† From the Department of Biochemistry, Texas Tech University, School of Medicine, Lubbock, Texas 79430. *Received August 25, 1978; revised manuscript received March 5, 1979.* This work was supported by Grant D-676 from the Robert A. Welch Foundation.

‡ On temporary leave from the Faculty of Pharmacy and Biochemistry, University of Zagreb, Croatia, Yugoslavia.

0006-2960/79/0418-2668$01.00/0